

IFUSP-DFN/02-078

Determining the oscillation parameters by Solar neutrinos and KamLAND

H. Nunokawa^{1,*} W. J. C. Teves^{2,†} and R. Zukanovich Funchal^{2‡}

¹ *Instituto de Física Teórica, Universidade Estadual Paulista,
Rua Pamplona 145, 01405-900 São Paulo, Brazil*

² *Instituto de Física, Universidade de São Paulo C. P. 66.318, 05315-970 São Paulo, Brazil*

Abstract

The neutrino oscillation experiment KamLAND has given the first evidence for disappearance of $\bar{\nu}_e$ coming from nuclear reactors. We have combined their data with all the solar neutrino data assuming two flavor neutrino mixing and obtained allowed parameter regions which are compatible with the so-called large mixing angle solution to the solar neutrino problem. The allowed regions in the plane of mixing angle and mass squared difference are now split into two islands at 99% C.L. We have speculated how these two islands can be separated in the near future. We have shown that a 50% reduction of the error on SNO neutral-current measurement can be important in establishing in each of these islands the true values of these parameters lie. We also have simulated KamLAND positron energy spectrum after 1 year of data taking, assuming the current best fitted values of the oscillation parameters, combined it the with current solar neutrino data and showed how these two split islands can be modified.

PACS numbers: 26.65.+t,13.15.+g,14.60.Pq,91.35.-x

*Electronic address: nunokawa@ift.unesp.br

†Electronic address: teves@charme.if.usp.br

‡Electronic address: zukanov@if.usp.br

I. INTRODUCTION

Many solar and atmospheric neutrino experiments have collected data in the last decades which can be interpreted as evidences that neutrinos produced in the Sun and in the Earth's atmosphere suffer flavor conversion. While the atmospheric neutrino results [1] may be understood assuming $\nu_\mu \rightarrow \nu_\tau$ conversion driven by a neutrino mass squared difference within the experimental reach of the K2K accelerator experiment [2], the mass squared differences needed to explain the solar neutrino data were until quite recently [3] too small to be inspected by a terrestrial neutrino oscillation experiment.

A number of different fits assuming standard neutrino oscillations induced by mixing and mass [4] as well as other exotic flavor conversion mechanisms [5] have been performed using the combined solar neutrino data from Homestake [6], Gallex/GNO [8, 9], SAGE [10], Super-Kamiokande-I [11] and SNO [12]. These analyses selected some allowed areas in the free parameter region of each investigated mechanism but did not allow one to establish beyond reasonable doubt which is the mechanism and what are the values of the parameters that are responsible for solar ν_e flavor conversion. After the first result of KamLAND (KL) [3] this picture has changed drastically.

In the first part of this paper, we present the allowed region for the oscillation parameters in two generations for the entire set of solar neutrino data, for KamLAND data alone and for KamLAND result combined with all solar neutrino data, showing that this last result finally establishes the large mixing angle (LMA) as the final solution to the solar neutrino problem, definitely discarding all the other mass induced or more exotic solutions. In the second part, we speculate on the possibility of further constraining the oscillation parameters in the near future. For instance, we point out the importance of SNO neutral-current (NC) data in further constraining the LMA solution. In particular, we discuss the consequence of a significant reduction (50 %) of the SNO neutral-current data uncertainty. Finally, we simulate the expected inverse β -decay e^+ energy spectrum for 1 year of KamLAND data, based on the best fitted values of the oscillation parameters. We combine this with the current solar neutrino data in order to show how the allowed parameter regions can be modified.

II. DETERMINATION OF OSCILLATION PARAMETERS

KamLAND has observed a suppression of the expected $\bar{\nu}_e$ flux in the absence of oscillation of about 61%, which is compatible with neutrino oscillations in two generations [3]. In this case the relevant oscillation parameters, which must be determined by the fit to experimental data, are Δm^2 and $\tan^2 \theta$. We first calculated the allowed region for these parameters compatible with all solar neutrino experimental data, then with KamLAND data alone, and finally we combine these two sets of data.

A. Solar Neutrino Experiments

We have determined the parameter region allowed by the solar neutrino rates measured by Homestake [6], Gallex/GNO [8, 9], SAGE [10], Super-Kamiokande-I [11] and SNO (elastic scattering, charged-current and neutral-current reactions) [12] as well as by the Super-Kamiokande-I zenith spectrum shape, assuming neutrino oscillations in two generations.

We have compute the $\nu_e \rightarrow \nu_e$ survival probability, properly taking into account the neutrino production distributions in the Sun according to the Standard Solar Model [13], the zenith-angle exposure of each experiment, as well as the Earth matter effect as in Ref. [5], except that here we solved the evolution equation entirely numerically. We then estimate the allowed parameter regions by a χ^2_{\odot} minimization.

In Figure 1 we show the region in the $(\tan^2 \theta, \Delta m^2)$ plane allowed by the rates of all solar neutrino experiments as well as by the Super-Kamiokande-I zenith spectrum at 90%, 95%, 99% and 99.73% C.L. In our fit we obtained a $\chi^2_{\odot}(\text{min}) = 37.7$ for 47 d.o.f (83 % C.L.), corresponding to the global best fit values $\Delta m^2 = 7.5 \times 10^{-5}$ eV² and $\tan^2 \theta = 0.42$.

B. KamLAND

KamLAND [3] is a reactor neutrino oscillation experiment searching for $\bar{\nu}_e$ oscillation from over 16 power reactors in Japan and South Korea which are mostly located at distances that vary from 80 to 344 km from the Kamioka mine, allowing KamLAND to probe the LMA neutrino oscillation solution to the solar neutrino problem.

The KamLAND detector consists of about 1 kton of liquid scintillator surrounded by

photomultiplier tubes that registers the arrival of $\bar{\nu}_e$ through the inverse β -decay reaction $\bar{\nu}_e + p \rightarrow e^+ + n$, by measuring e^+ and the 2.2 MeV γ -ray from neutron capture of a proton in delayed coincidence. The e^+ annihilate in the detector producing the total visible energy E which is related to the incoming $\bar{\nu}_e$ energy, E_ν , as $E = E_\nu - (m_n - m_p) + m_e$, where m_n , m_p and m_e are respectively the neutron, proton and electron mass.

After 145.1 days of data taking, which correspond to 162 ton yr exposure, KamLAND has measured 54 inverse β -decay events where 87 were expected without neutrino conversion, distributed in 13 bins of 0.425 MeV above the analysis threshold of 2.6 MeV applied to contain the background under about 1 event.

We have theoretically computed the expected number of events the i -th bin, N_i^{theo} , as

$$N_i^{\text{theo}} = \int dE_\nu \sigma(E_\nu) \sum_k \phi_k(E_\nu) P_{\nu_e \rightarrow \nu_e} \int_i dE R(E, E'),$$

where $R(E, E')$ is the energy resolution function, E the observed and E' the true e^+ energy, with the energy resolution $7.5\%/\sqrt{E(\text{MeV})}$. Here $\sigma(E_\nu)$ is the neutrino interaction cross-section and ϕ_k is the neutrino flux from the k -th power reactor, we have included all reactors with baseline smaller than 350 km in the sum, $P_{\nu_e \rightarrow \nu_e} \equiv P_{\bar{\nu}_e \rightarrow \bar{\nu}_e}$ (if CPT is conserved, which we will assume here) is the familiar neutrino survival probability in vacuum, which is equal to one in case of no oscillation, and explicitly depend on Δm^2 and $\tan^2 \theta$.

We were able to compute the regions in the $(\tan^2 \theta, \Delta m^2)$ plane allowed by KL data by minimizing with respect to these free parameters, the χ^2_{KL} function defined as $\chi^2_{\text{KL}} = \chi^2_{\text{G}} + \chi^2_{\text{P}}$ with

$$\chi^2_{\text{G}} = \sum_i \frac{(N_i^{\text{theo}} - N_i^{\text{obs}})^2}{\sigma_i^2},$$

and

$$\chi^2_{\text{P}} = \sum_j 2(N_j^{\text{theo}} - N_j^{\text{obs}}) + 2 N_j^{\text{obs}} \ln \frac{N_j^{\text{obs}}}{N_j^{\text{theo}}},$$

where $\sigma_i = \sqrt{N_i^{\text{obs}} + (0.0642 N_i^{\text{obs}})^2}$ is the statistical plus systematic uncertainty in the number of events in the i -th bin and the sum in $i(j)$ is done over the bins having 4 or more (less than 4) events.

Using this χ^2_{KL} we have computed the allowed regions at 90%, 95%, 99% and 99.73% C.L. shown in Fig. 2. In our fit we obtained a $\chi^2_{\text{KL}}(\text{min}) = 5.4$ for 11 d.o.f (91 % C.L.),

corresponding to the best fit values $\Delta m^2 = 7.0 \times 10^{-5}$ eV 2 and $\tan^2 \theta = 0.79$.

C. Combined Results

Combining the results of all solar experiments with KamLAND data we have obtained the allowed regions showed in Fig. 3. The minimum value of $\chi^2_{\text{tot}} = \chi^2_{\odot} + \chi^2_{\text{KL}}$ for the combined fit is $\chi^2_{\text{tot}}(\text{min}) = 43.6$ for 60 d.o.f (94.5 % C.L.), corresponding to the best fit values $\Delta m^2 = 7.1 \times 10^{-5}$ eV 2 and $\tan^2 \theta = 0.42$. We observe that there are two separated regions which are allowed at 99 % C.L.: a lower one in Δm^2 (region 1) where the global best fit point is located, and an upper one (region 2) where the local best fit values are $\Delta m^2 = 1.5 \times 10^{-4}$ eV 2 and $\tan^2 \theta = 0.41$, corresponding to $\chi^2_{\text{loc}}(\text{min}) = 49.2$. We observe that depending on the definition of χ^2_{KL} used there appear at 99.73% C.L. a third region above $\Delta m^2 = 2 \times 10^{-4}$ eV 2 .

In Fig. 4 we show the theoretically predicted energy spectra at KamLAND for no oscillation, the best fit values of the oscillation parameters for KamLAND data alone and for KamLAND combined with solar data in regions 1 and 2. We note that the fourth energy bin, which is for the moment below the analysis cut can be quite important in determining the value of the oscillation parameters in the future.

III. FUTURE PERSPECTIVES

In this section we consider the effect of possible future experimental improvements which can help in determining the oscillation parameters. We first consider a reduction of the error in SNO neutral-current measurement then an increase of the event statistics in KamLAND.

A. Effect of reducing SNO neutral-current error

In order to constrain the solar neutrino oscillation parameters even more, in particular, to decide in which of the 99% C.L. islands Δm^2 really lie, we have investigated the effect of increasing the SNO neutral-current data precision to twice its current value. We have re-calculated the region in the $(\tan^2 \theta, \Delta m^2)$ plane allowed by all current solar neutrino data artificially decreasing the SNO error but keeping the current central value, as well as

the other solar neutrino data unchanged. The result can be seen in Fig. 5. The best fit point and the value of $\chi^2_{\odot}(\text{min})$ remain practically unchanged with respect to the result obtained in Sec. II A, but the allowed region shrinks significantly. This is because the 8B flux normalization, which can be directly inferred by SNO NC measurements, gets more constrained. Combining this with KamLAND data we obtain the allowed region shown in Fig. 6. We observe that this allowed region is substantially smaller compared to the one shown in Fig. 3. Moreover, region 2 only remains at 99 % C.L.

B. Effect of increasing KamLAND statistics

We simulate the expected KamLAND spectrum after one year of data taking for three distinct assumptions. We have generated KamLAND future data compatible with the best fitted values of Δm^2 and $\tan^2 \theta$ obtained for : (a) KamLAND data alone, (b) KamLAND and current solar neutrino data in region 1 and (c) KamLAND and current solar neutrino data in region 2. We have also included an extra bin, corresponding to the fourth bin in Fig. 4. We have re-calculated the region allowed by the combined fit with the current solar neutrino data in each case.

The results of our calculations can be seen in Fig. 7-9. If the future KamLAND result is close to the current one (see Fig. 7), values of $\tan^2 \theta$ larger than the ones allowed now will be possible and region 2 will be excluded at 99% C.L. For this case we have obtained $\chi^2_{\text{tot}}(\text{min}) = 42.1$. On the other hand, if the future KamLAND data are more compatible with the current best fit point of solar neutrino data (see Fig. 8), the global allowed region will diminish substantially with respect to Fig. 3 and region 2 will only remain at 99% C.L. For this case we have obtained $\chi^2_{\text{tot}}(\text{min}) = 39.1$. Finally, if after one year KamLAND data is more compatible with region 2 (see Fig. 9) then one should observe an increase towards larger values of Δm^2 in the combined allowed region with respect to the one shown in Fig. 3. In this case region 1 and 2 will have similar statistical significance, corresponding to $\chi^2_{\text{tot}}(\text{min}) \sim 44.0$.

IV. DISCUSSIONS AND CONCLUSION

We have performed a combined analysis of the complete set of solar neutrino data with the recent KamLAND result in a two neutrino flavor oscillation scheme. We have obtained, in agreement with other groups [14], two distinct islands, denominated regions 1 and 2, in the $(\tan^2 \theta, \Delta m^2)$ plane which are the most probable regions where the true values of these parameters lie. Region 1, where the global best fit point was found, is around $\Delta m^2 = 7.1 \times 10^{-5}$ eV 2 , while region 2 is around $\Delta m^2 = 1.5 \times 10^{-4}$ eV 2 .

We have considered two possible improvements in the determination of the neutrino oscillation parameters in the future. First we have investigated the effect of a decrease of 50 % in the error of the SNO NC measurement. We have shown that this will substantially decrease the allowed parameter region when combined with KamLAND data. In particular, region 2 would not be allowed at 95% C.L. anymore.

Second we have studied what can happen in the near future, when KamLAND collects 1 year of data. We have simulated the expected KamLAND spectrum including an extra lower bin, corresponding to the fourth bin in Fig. 3. Three difference cases were studied in combination with the present solar neutrino data. In the first case we assumed the future KamLAND spectrum will be compatible with oscillation parameter values at the best fit point for the present KamLAND data alone. This is the most restrictive case for region 2. In the second case we have considered that future data will be more compatible with the present best fit point of the solar neutrino experiments. In this case the combined allowed region will be much smaller the present one and region 2 will be only allowed at 99 % C.L. Finally, in the third case, we have assumed that in the future KamLAND data will be compatible with the local best fit point in region 2. In this case the combined allowed region will suffer an increase towards larger values of Δm^2 and region 1 and 2 will both remain with similar statistical significance.

Acknowledgments

This work was supported by Fundação de Amparo à Pesquisa do Estado de São Paulo (FAPESP), Conselho Nacional de Ciência e Tecnologia (CNPq).

- [1] Super-Kamiokande Collaboration, Y. Fukuda *et al.*, Phys. Rev. Lett. **81**, 1562 (1998); Kamiokande Collaboration, H. S. Hirata *et al.*, Phys. Lett. B **205**, 416 (1988); *ibid.* **280**, 146 (1992); Y. Fukuda *et al.*, *ibid.* **335**, 237 (1994); IMB Collaboration, R. Becker-Szendy *et al.*, Phys. Rev. D **46**, 3720 (1992); MACRO Collaboration, M. Ambrosio *et al.*, Phys. Lett. B **478**, 5 (2000); B. C. Barish, Nucl. Phys. B (Proc. Suppl.) **91**, 141 (2001); Soudan-2 Collaboration, W. W. M. Allison *et al.*, Phys. Lett. B **391**, 491 (1997); Phys. Lett. B **449**, 137 (1999); W. A. Mann, Nucl. Phys. B (Proc. Suppl.) **91**, 134 (2001).
- [2] K2K Collaboration, S. H. Ahn *et al.*, Phys. Lett. B **511**, 178 (2001); arXiv:hep-ex/0212007.
- [3] KamLAND Collaboration, K. Eguchi *et al.*, arXiv:hep-ex/0212021; see also <http://www.awa.tohoku.ac.jp/KamLAND/index.html>.
- [4] J. N. Bahcall, M. C. Gonzalez-Garcia and C. Peña-Garay, JHEP **0207**, 054 (2002) [arXiv:hep-ph/0204314]; A. Bandyopadhyay, S. Choubey, S. Goswami and D. P. Roy, Phys. Lett. B **540**, 14 (2002) [arXiv:hep-ph/0204286]; V. Barger, D. Marfatia, K. Whisnant and B. P. Wood, Phys. Lett. B **537**, 179 (2002) [arXiv:hep-ph/0204253]; P. Aliani, V. Antonelli, R. Ferrari, M. Picariello and E. Torrente-Lujan, arXiv:hep-ph/0211062; P. C. de Holanda and A. Y. Smirnov, arXiv:hep-ph/0205241; P. Creminelli, G. Signorelli and A. Strumia, JHEP **0105**, 052 (2001) [arXiv:hep-ph/0102234]; G. L. Fogli, E. Lisi, A. Marrone, D. Montanino and A. Palazzo, Phys. Rev. D **66**, 053010 (2002) [arXiv:hep-ph/0206162]; M. Maltoni, T. Schwetz, M. A. Tortola and J. W. F. Valle, arXiv:hep-ph/0207227.
- [5] A. M. Gago, M. M. Guzzo, P. C. de Holanda, H. Nunokawa, O. L. Peres, V. Pleitez and R. Zukanovich Funchal, Phys. Rev. D **65**, 073012 (2002) [arXiv:hep-ph/0112060], and references therein.
- [6] Homestake Collaboration, B. T. Cleveland *et al.*, Astrophys. J. **496**, 505 (1998).

- [7] Kamiokande Collaboration, Y. Fukuda *et al.*, Phys. Rev. Lett. **77**, 1683 (1996).
- [8] GALLEX Collaboration, W. Hampel *et al.*, Phys. Lett. B **447**, 127 (1999).
- [9] GNO Collaboration, M. Altmann *et al.*, Phys. Lett. B **490**, 16 (2000); C. Cattadori on behalf of GNO Collaboration, talk presented at TAUP2001, 8-12 September 2001, Laboratori Nazionali del Gran Sasso, Assergi, Italy.
- [10] SAGE Collaboration, D. N. Abdurashitov *et al.*, Nucl. Phys. (Proc. Suppl.) **91**, 36 (2001); Latest results from SAGE homepage: <http://EWIServer.npl.washington.edu/SAGE/>.
- [11] SuperKamiokande Collaboration, S. Fukuda *et al.*, Phys. Lett. B **539**, 179 (2002).
- [12] SNO Collaboration, Q. R. Ahmad *et al.*, Phys. Rev. Lett. 87, 071301 (2001); *ibid.* **89**, 011301 (2002); **89**, 011302 (2002).
- [13] J. N. Bahcall, M. H. Pinsonneault and S. Basu, Astrophys. J. **555**, 990 (2001).
- [14] V. Barger and D. Marfatia, arXiv:hep-ph/0212126; G. L. Fogli, *et al.*, arXiv:hep-ph/0212127; M. Maltoni, T. Schwetz and J. W. F. Valle, arXiv:hep-ph/0212129; A. Bandyopadhyay, *et al.*, arXiv:hep-ph/0212146; J. N. Bahcall, M. C. Gonzalez-Garcia and C. Peña-Garay, arXiv:hep-ph/0212147.

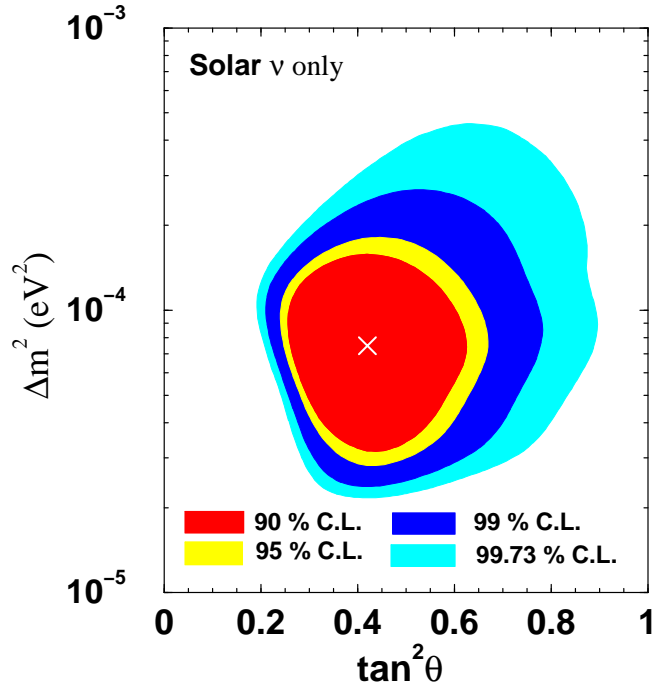


FIG. 1: Region in $(\tan^2 \theta, \Delta m^2)$ plane allowed by the Super-Kamiokande-I zenith spectrum combined with rates from Homestake, Gallex/GNO, SAGE and SNO. The best fit point is marked by a cross.

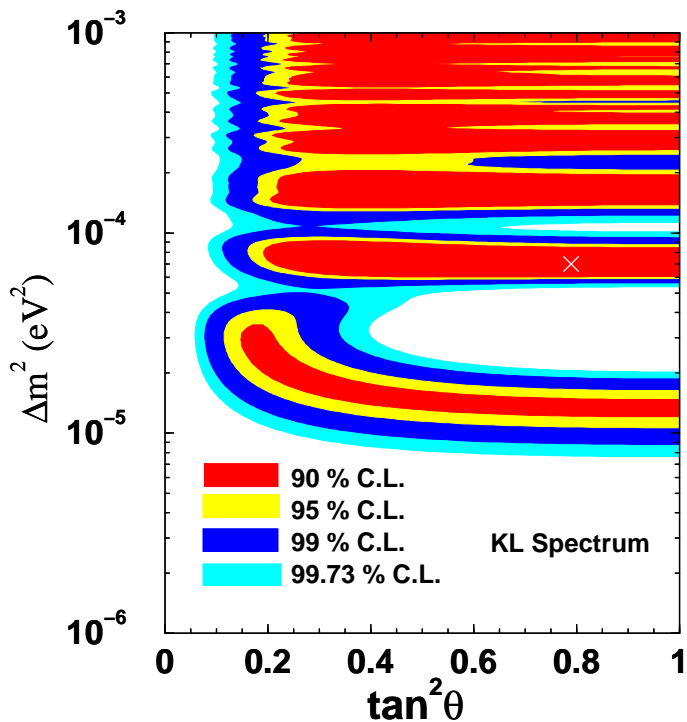


FIG. 2: Regions in $(\tan^2 \theta, \Delta m^2)$ plane allowed by KL data alone. The best fit point is marked by a cross.

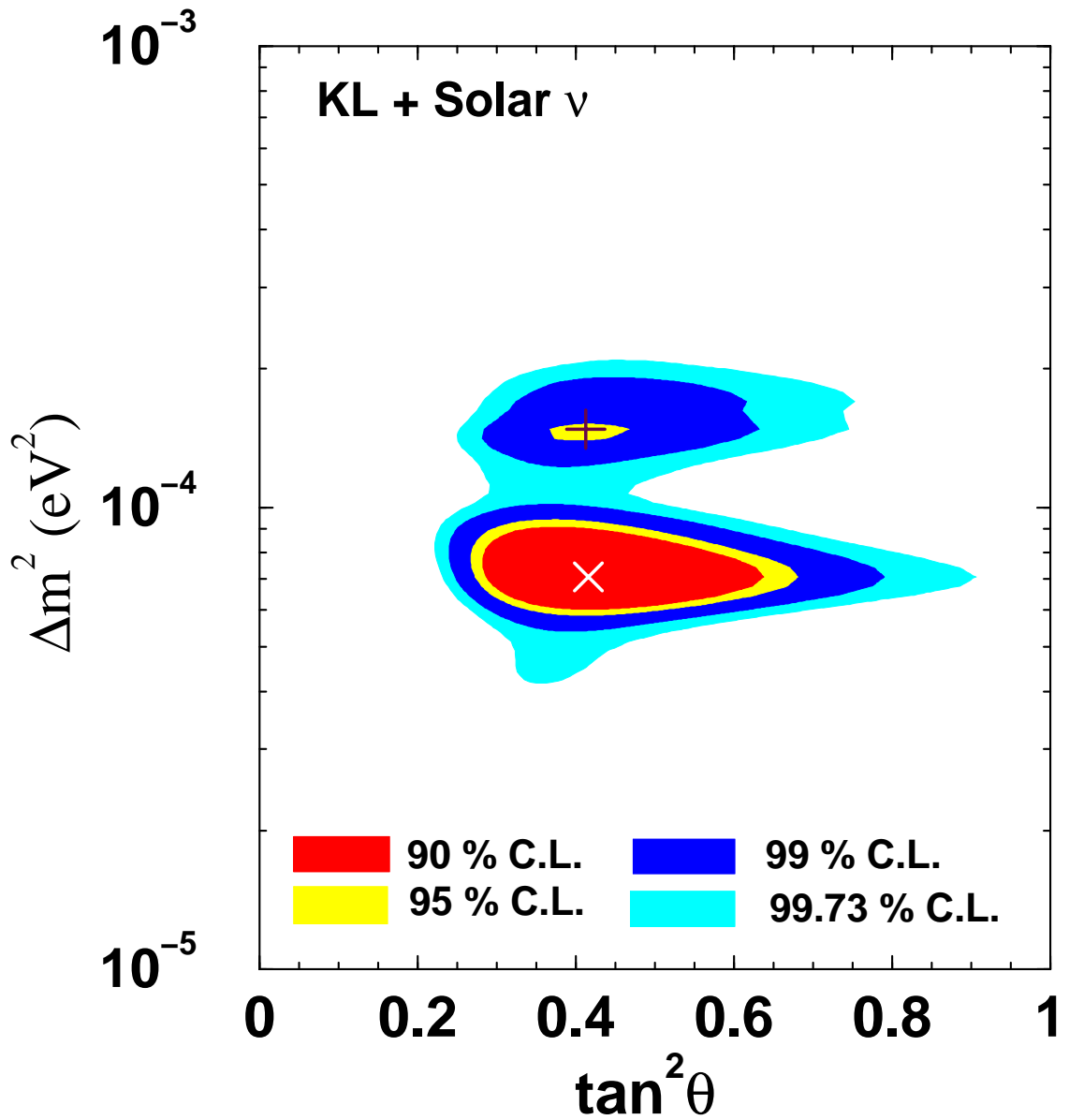


FIG. 3: Region allowed by all the solar neutrino experiments combined with KL data. The region below (above) $\Delta m^2 = 10^{-4}$ eV² is referred to as region 1 (2). The best fit points in each region are also marked by cross and plus.

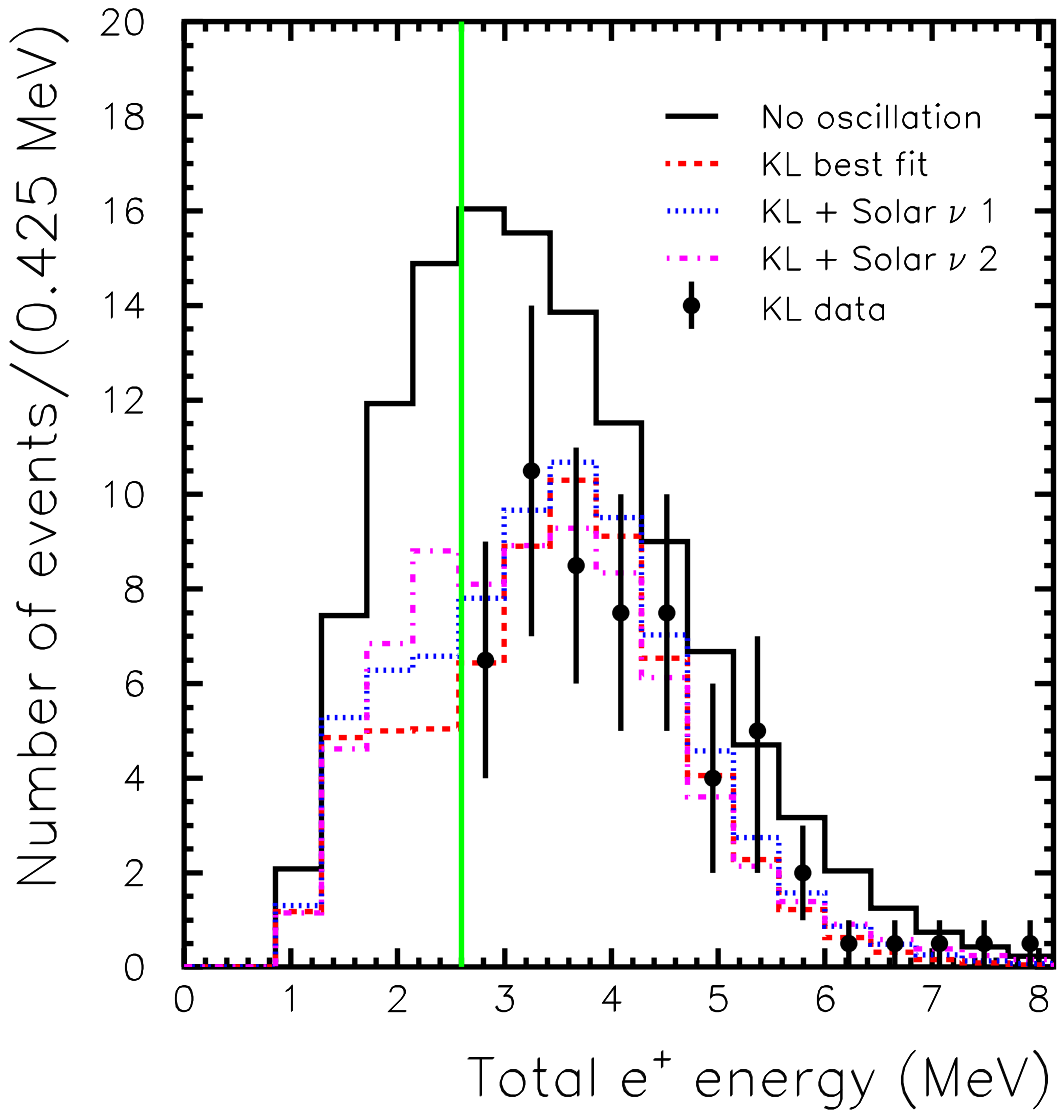


FIG. 4: Expected energy spectra for no oscillation, the best fit values of the oscillation parameters for KL data alone and KL data combined with the solar neutrino data in regions 1 and 2 of Fig. 3. The KL data [3] is also shown as solid circles with error bars. The energy threshold at 2.6 MeV is marked by a vertical line.

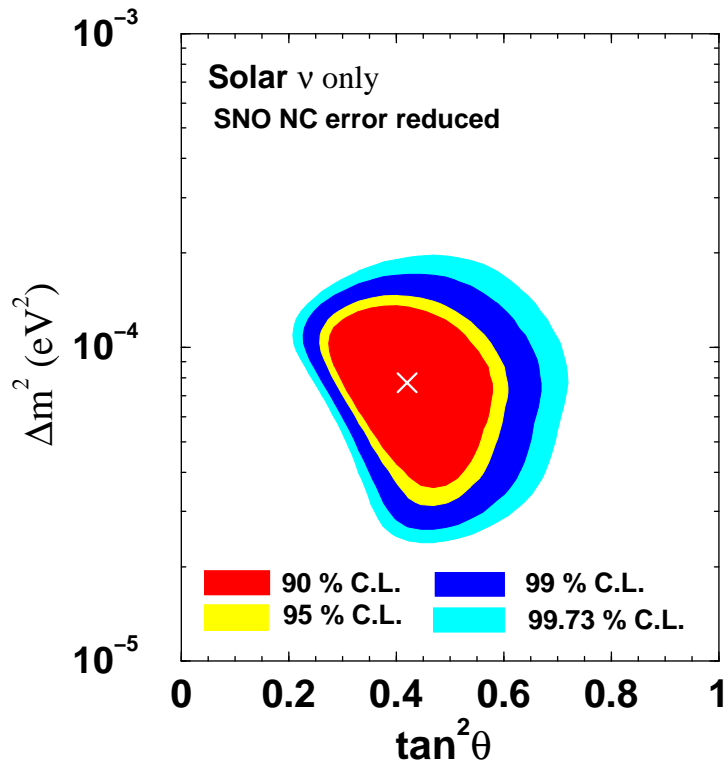


FIG. 5: Same as Fig. 1 but decreasing the SNO neutral-current data error to half its current value.

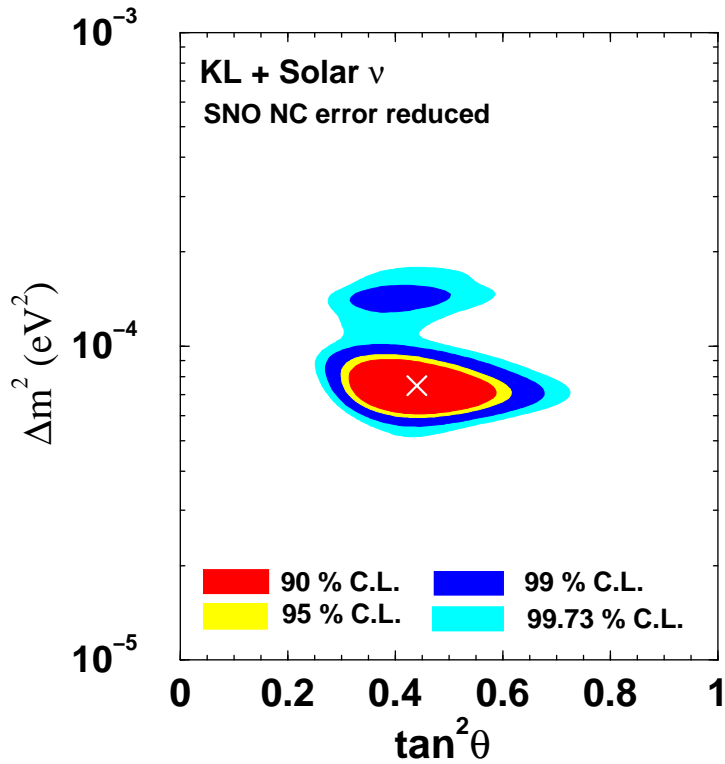


FIG. 6: Same as Fig. 3 but decreasing the SNO neutral-current data error to half its current value.

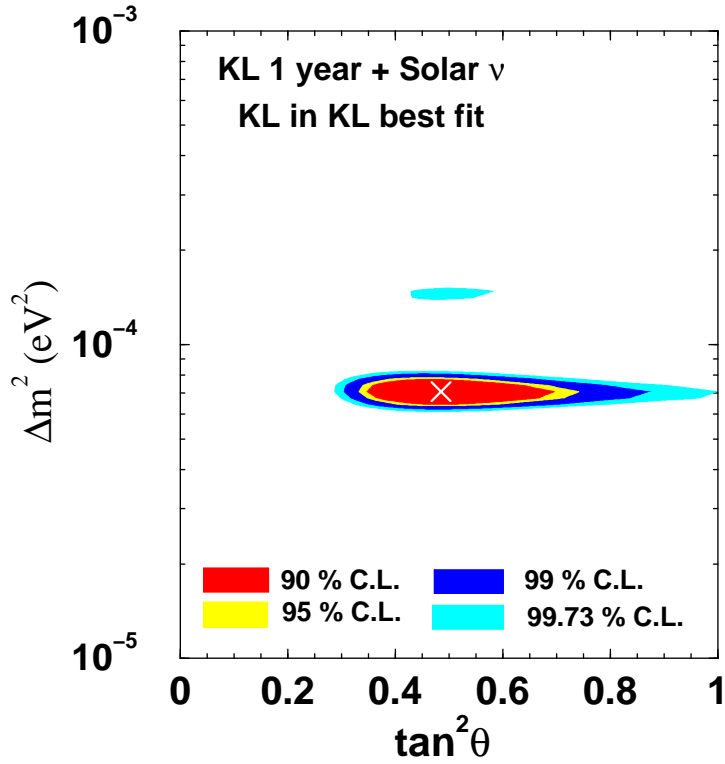


FIG. 7: Same as Fig. 3 but for a simulated KamLAND spectrum after one year of data taking compatible with $\Delta m^2 = 7 \times 10^{-5}$ eV² and $\tan^2 \theta = 0.79$.

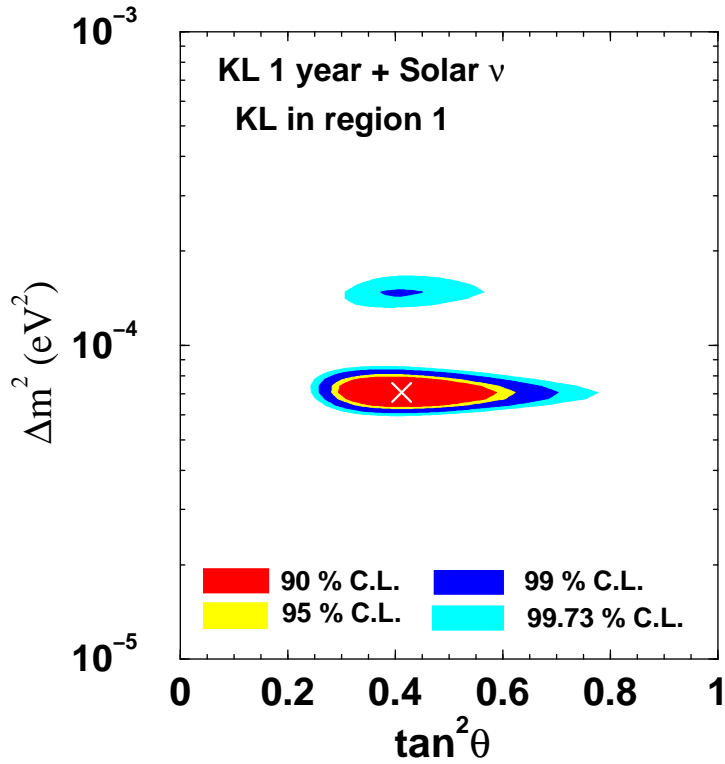


FIG. 8: Same as Fig. 7 but for $\Delta m^2 = 7.1 \times 10^{-5}$ eV² and $\tan^2 \theta = 0.42$.

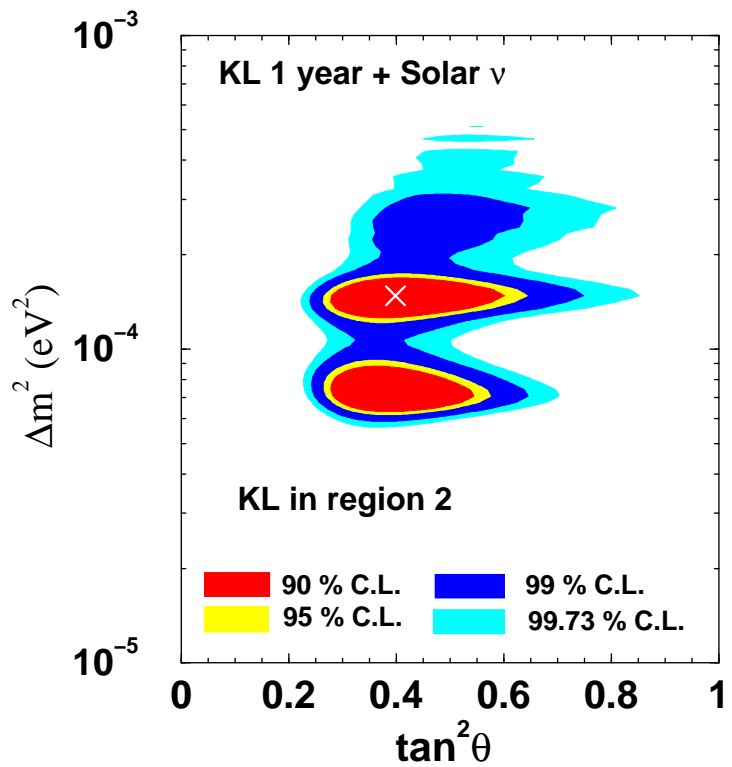


FIG. 9: Same as Fig. 7 but for $\Delta m^2 = 1.5 \times 10^{-4}$ eV 2 and $\tan^2 \theta = 0.41$.